# A method to estimate concrete hydraulic conductivity of underground tunnel to assess lining degradation

Paola Bagnoli [a,*,1], Mirko Bonfanti [a,1], Gabriele Della Vecchia [b,1], Maurizio Lualdi [b], Luca Sgambi [b]

[a] *Department of Chemistry, Materials and Chemical Engineering "Giulio Natta", Politecnico di Milano, Piazza Leonardo da Vinci 32, 20133 Milan, Italy*
[b] *Department of Civil and Environmental Engineering, Politecnico di Milano, Piazza Leonardo da Vinci 32, 20133 Milan, Italy*

Received 2 December 2014
Received in revised form 20 May 2015
Accepted 12 August 2015

## 1. Introduction

Mechanical and hydraulic characteristics of concrete tunnel linings undergo significant changes during the life-time of the infrastructure. Long-term structural assessment is thus one of the key activities in monitoring and maintaining the performance of a tunnel during its service life (Usman and Galler, 2013). Recently, the owners of underground infrastructures have started to become concerned about tunnel life expectancy: some structures, designed for a lifetime of about 100 years, are now beginning to approach such an age (Vanicek and Vanicek, 2007). Due to the interaction with the surrounding environment, the lining of a tunnel is indeed subjected to mechanical, physical, chemical and biological actions of various agents that may accelerate the degradation process of the concrete constituting the structure (Kuhl et al., 2004a,b). In particular, the detailed design, concrete production and placing, applied curing and post curing exposure, and operating environment all impact on concrete linings durability. More in detail, whilst designing an underground concrete structure it must be considered that the durability of the concrete is strongly affected by operational environment, shape and bulk of the concrete, cover to embedded steel, type of cement, type of aggregates, type and dosage of admixture, cement content and free water cement ratio, as well as permeability, porosity and diffusivity of the final concrete (BTS and ICE, 2004). According to the Tunnel Lining Design Guide provided by the British Tunnelling Society (BTS and ICE,

* Corresponding author.
*E-mail address:* paola.bagnoli@polimi.it (P. Bagnoli).
[1] These authors equally contributed to this paper.

2004), the main factors of attack that reduce the durability of concrete involves the corrosion of metals; the chloride-induced and carbonation-induced corrosion of embedded metals, sulphate attack, acid attack and alkali-silica reaction. It is thus evident that the evolution of lining properties not only depends on the materials involved, but also on the environmental conditions, on the type of degradation process and, obviously, on time. With reference to sprayed concrete (shotcrete) lining, Usman and Galler (2013) highlighted that, under the influence of different deterioration processes, the shotcrete support loses its characteristics and may become unable to fully support the structure in the long term. The impact on the tunnel structural stability has been tackled by Usman and Galler (2013) via numerical simulations which accounts for reduction in concrete stiffness and strength proper-ties. Reinforced concrete strength evolution of tunnel lining under corrosion conditions has been also tackled by Zhiquiang and Mansoor (2013).

When the tunnel is submerged, the presence of cracks and fissures related to concrete deterioration, as well as changes in lining thickness, can significantly influence the seepage of underground water. The consequence of the increasing lining hydraulic conductivity is twofold, especially if a drainage system was not provided for. On the one hand, unexpected water inflow in a tunnel can cause several problems in terms of the working activity of the infrastructure, i.e. forced interruption of railway or metro traffic if the groundwater level rise up to a critical level. On the other hand, when groundwater starts to flow into the tunnel, seepage forces start to act on the cross-section of the tunnel, influencing the structural safety of the infrastructure. The effect of seepage forces acting on the tunnel lining has been highlighted by Lee and Nam (2001) for shallow drainage-type tunnels, whilst the influence of seepage forces on the tunnel ground reaction curve was tackled by Lee et al. (2006) and Shin et al. (2010).

Despite crucial for infrastructure owners, the determination of the current degradation state of their underground structures and of the potential risks related to aging processes is still a complex and often expensive task. For example, for the monitoring of structural properties of the lining of the Prague Metro, geophysical system using MEMS sensors have been implemented and two different techniques are used: seismic velocity sampling and the analysis of the time-dependent frequency spectra of structure vibra-tion under traffic load (Machacek and Bartak, 2003). A different approach is here proposed, which relies on the coupling of numerical analysis of tunnel water inflow rates and experimental data in order to estimate concrete hydraulic properties. The permeability of the concrete is indeed proposed as a proxy of the overall degradation state of the structure. This assumption lies on the evidence that the hydraulic conductivity of a porous medium, like concrete, depends on its porosity and it is dramatically affected by the pres-ence of fissures and fractures and their interconnections (Choinska et al., 2007). According to Pijaudier-Cabot et al. (2009), the evolution of permeability of concrete with cracking may be described by two fundamentally different modelling approaches: on one hand, the permeability can be viewed as a function of continuum damage based variable, able to capture the diffuse microcracks. On the other hand, when microcracking has localised to form a macrocrack, the permeability can be modelled as a function of the opening, the con-nectivity and the tortuosity of the cracks. In this case, Poiseuille flow is the most common assumption. According to experimental results, the transition between these two descriptions is progressive, due to the non-sudden (if the concrete is compressed) mechanical transi-tion between diffused microcracking and their coalescence to form a macrocrack. Discrete approaches to crack propagation and to fluid flow in fractured media, along with multiscale modelling, provide a possible connection between flow inside existing discontinuities and the overall macroscopic governing equations for a porous medium (e.g. Rèthorè et al., 2007). However, due to the need of an extremely accurate microcraking characterisation, of the discretiza-tion difficulties associated with these approaches and of the heavy computational effort, for the sake of simplicity and to allow the application of the method also if few data are available, we decided to follow a simple phenomenological continuum approach. In this case, porosity is used as a scalar damage variable and it is thus assumed to be the primary parameter affecting hydraulic conductiv-ity. Coherently with the approach proposed, the state of deteriora-tion of the infrastructure can be assessed by monitoring the evolution of hydraulic conductivity: as long as the deterioration pro-ceeds, the hydraulic conductivity of the concrete will increase.

Neglecting the possibility of measuring the hydraulic conductivity of the lining concrete by direct methods, which should involve core sampling, an indirect non-destructive approach is here proposed. Provided the availability of experimental measure-ments of water inflow in the tunnel and the knowledge of the position of the water table, the hydraulic conductivity of concrete can be estimated by means of an inverse analysis process performed by a numerical approach.

Being the water inflow in a tunnel also a function of the effective geometry of the underground structure, the thickness of the concrete lining is an important factor to be considered too. To this aim, an integrated approach is here suggested, exploiting non-destructive techniques as Ground Penetrating Radar (GPR)(Daniels, 2004) to gain information about actual tunnel thickness. Geophysical data are subsequently used as an input for an ad hoc implemented finite element model to quantitatively estimate concrete hydraulic conductivity.

The experimental data reported in this paper and used as model input, as well as the data used for the validation, refer to measurements performed on a real underground tunnel. However, the proposed method can be considered of general validity: it can be easily extended for the study of any underground tunnel once some geometrical features of the tunnel and the hydraulic properties of the surrounding soil are provided (i.e. the thickness of the concrete lining, the position of the tunnel with respect to the ground surface and to the water table).

It is worth noting that the method is intended as a tool for the estimate of the global degradation state of a tunnel, in order to help the owners of underground infrastructures to fix the most critical sections depending on the effective state and geometry of the lining, as well as on groundwater position.

## 2. Methods

### *2.1. Seepage model*

In order to allow the estimate of concrete hydraulic conductivity by means of inverse analysis, numerical simulations to evaluate water inflow into the tunnel need to be performed. Generally speaking, these predictions are burdened by a high level of uncertainty, with special reference to ground hydraulic properties, e.g. the highly inhomogeneous distribution of hydraulic conductivity in the ground (Kolymbas and Wagner, 2007). For this reason, and keeping in mind the purpose of the paper, the assumption of homogeneous and isotropic hydraulic conductivity of the soil is used as a first approximation.

A prediction of the groundwater inflow into a drained tunnel has been previously analytically obtained by Kolymbas and Wagner (2007), under the assumption of homogeneous and isotro-pic permeability of the soil, steady flow and circular tunnel cross section, held at constant hydraulic potential. However, this analytical solution holds only for completely submerged tunnels, which is often not the case for underground metro lines. In order to keep

the problem as general as possible, the case of a water table set at an intermediate level of the tunnel is here considered. In this case, the most general approach relies in considering the soil surrounding the tunnel as an unsaturated porous medium, i.e. whose degree of saturation Sr (volume of water over the volume of voids) can be lower than 1. The solution for the submerged tunnel is thus recovered as a particular case.

Due to the degradation of the tunnel lining, the concrete thickness may not be constant along the length of aged tunnels, thus the problem is intrinsically three-dimensional. However, for the sake of simplicity and to reduce computational effort, a pseudo 3D approach was here chosen. The seepage problem in each tunnel section was analysed as 2D, and the total water inflow along the tunnel was obtained as the sum of the contribution of each section (see Section 2.2 for further details).

*2.1.1. Geometry*

The cross-section of the considered tunnel is shown in Fig. 1a. Being the water inflow in the linings a function of both the hydraulic conductivity – which is expected to increases with damage- and the thickness of the concrete lining – which is supposed to reduce for increasing damage – the model has been set up to account for different grade of tunnel thickness degradation, by means of a parametric geometry in which the tunnel-section thickness is modifiable. In this way, the contribution of the most damaged zone to the calculated water inflow can be accounted for. According to GPR measurements, the parameter assumed to be influenced by damage is the thickness of the tunnel invert ($S_i$ in Fig. 1a). The value of $S_i$ ranged between 0.55 m, corresponding to the original thickness of the undamaged tunnel, and 0.1 m, in accordance with the geometrical data measured by GPR survey. Vice versa, the thickness of the crown and side parts of the tunnel was assumed to be constant (0.5 m), based on experimental visual inspection performed on the real tunnel which has shown no evident damage in these parts of the structure.

As for the soil surrounding the tunnel, the considered domain is a rectangle, whose width $W_d$ equals 100 m and whose height $H_d$ is 100 m. To avoid that the width of the soil domain can affect the outcomes of the simulations, the parameter $W_d$ was chosen considering the position of the piezometers used to measure the hydraulic head at a certain distance from the tunnel, to provide sound boundary conditions. The parameter $H_d$ was chosen based on experimental data reporting the depth of the impervious clay layer. According to the geometry of this specific case, the bottom part of the tunnel cross-section was placed 16.3 m deep with respect to the ground surface.

*2.1.2. GPR data*

The thickness of the concrete lining strongly affects the study of the seepage problem. To the aim of estimating lining thickness, GPR was exploited (Fig. 2a). GPR is a non-destructive technique, which allows detecting layers characterised by different electro-magnetic impedance and ensures a sufficient resolution to mea-sure thickness up to few centimetres (Daniels, 2004). GPR extensive measurements can be achieved quickly and not expen-sively. Preliminary tests were performed to select the best GPR configuration to avoid noise due to the presence of metallic materials in the tunnel (Lualdi and Lombardi, 2014a,b). Based on these tests, the chosen GPR antenna was the 600 MHz IDS antenna (IDS S. p.a., Pisa, Italy), to be used in the VV configuration (i.e. direction of the dipoles parallel to the direction of survey). A polyvinylchloride sledge was assembled with two 600 MHz IDS antennas: one in VV configuration, the other in HH configuration (i.e. direction of the dipoles perpendicular to the direction of survey). The HH antenna allowed to identify the hyperbole reflections generated by the cross metallic rebar of the concrete (Xiang et al., 2013). These hyperboles were compared with synthetic reflection hyperbole to derive the speed of electromagnetic waves and the thickness of the concrete layers was finally determined (resolution 0.03 m). In order to verify the reliability of GPR-based thickness estimation, nine core-samples were retrieved along the tunnel. The thickness of the core-samples was measured, obtaining a maximum differ-ence with respect to GPR measurements of about 0.03 m, thus con-firming the goodness of the GPR survey.

A quasi-continuous trend of the invert concrete thickness has finally been defined from GPR raw data along the length of the tunnel (acquisition step 0.02 m) (Fig. 2b).

This trend was then simplified in a discrete thickness distribution, adopted in the model to reduce the computational cost: the tunnel-invert thickness measurements (Fig. 2a) were subdivided into 5 classes (Fig. 2b), each one characterised by a mean value of the invert thickness ($S_i$ = 0.1, 0.2, 0.3, 0.4, and 0.5 m). The statis-tical frequency $X_{Si}$ of each class was calculated as the counts of the GPR measurements belonging to each class divided by the total number of the measurements. The overall tunnel length related

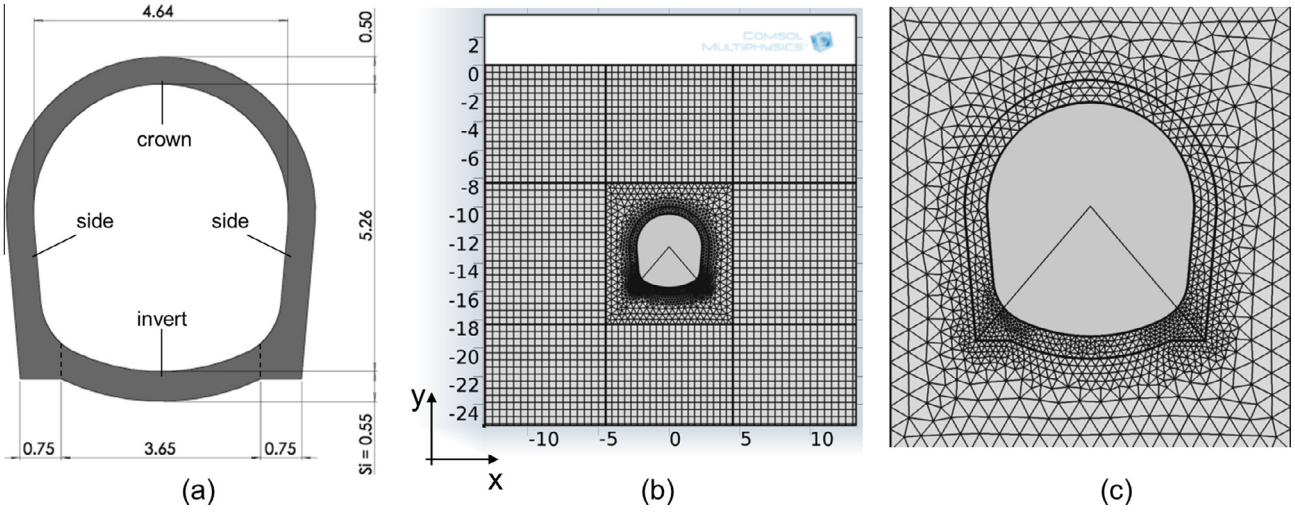


**Fig. 1.** Geometry of the model of underground tunnel: (a) cross-section of the tunnel (all dimensions are in meters); (b) mesh discretization of the computational domain; (c) detail of the unstructured mesh around the tunnel cross-section.

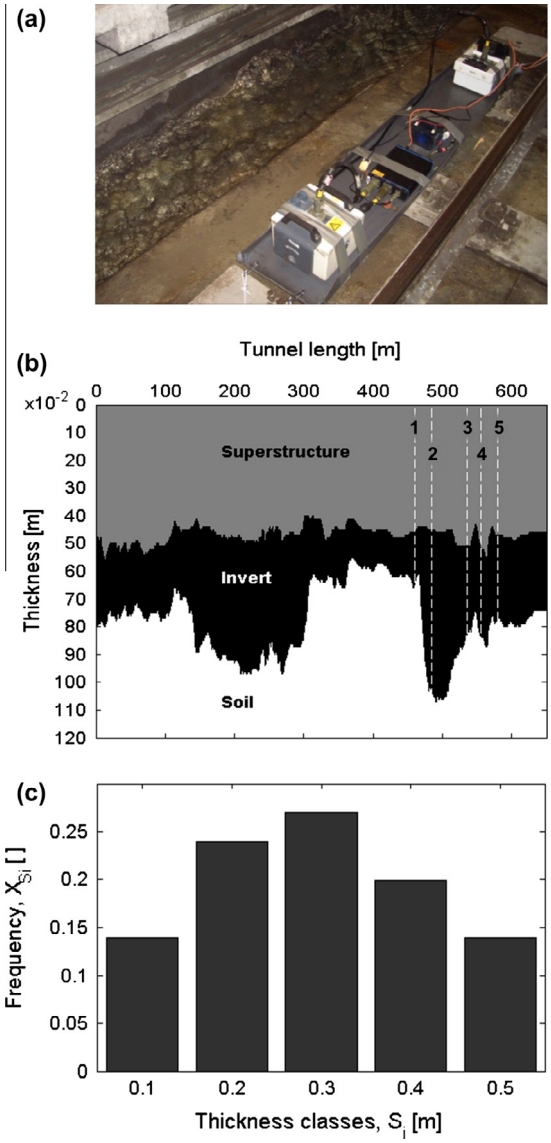


**Fig. 2.** In situ measurement of the thickness of the underground tunnel: (a) Ground penetrating Radar apparatus; (b) local thickness of the invert (in black) from GPR data. The dashed lines indicate the position of the core samples used for MIP testing; (c) discrete distribution of the invert thickness considered in the model. The frequency of each thickness class ($S_i$) along the tunnel is expressed as a fraction $X_{Si}$ of the total length of the tunnel.

to each thickness class $L_{Si}$ is calculated as $L_{Si} = L_{TOT} \cdot X_{Si}$ where $L_{TOT}$ is the total length of the tunnel ($L_{TOT}$ = 650 m) (Table 1).

*2.1.3. Model formulation*

For the purpose of this paper, both soil and concrete have been modelled as porous media with rigid solid skeleton. In order to simulate the unconfined problem of the seepage of water in the tunnel, the water mass balance equation of an unsaturated porous medium was considered. Under the assumption of incompressible pore water, the water mass balance equation reads

$$\phi \frac{\partial Sr}{\partial t} + \nabla \cdot \mathbf{v}_w = 0, \tag{1}$$

where $\phi$ is the porosity (volume of voids over the total volume of the porous medium), $Sr$ is the degree of saturation (volume of pore water over the volume of voids) and $\mathbf{v}_w$ is the specific discharge of water (i.e. discharge per unit area of the porous medium). In order

**Table 1**
Concrete lining thickness distribution.

| $S_i$ (m) | $X_{Si}$ () | $L_{Si}$ (m) |
|---|---|---|
| 0.1 | 0.14 | 90 |
| 0.2 | 0.24 | 159 |
| 0.3 | 0.27 | 178 |
| 0.4 | 0.20 | 131 |
| 0.5 | 0.14 | 92 |

$S_i$ is the invert thickness class.
$X_{Si}$ is the statistical frequency of the thickness measurements belonging to each $S_i$.
$L_{Si}$ is the total tunnel length belonging to each class: $L_{Si} = L_{TOT} \cdot X_{Si}$, where $L_{TOT}$ = 650 m is the total length of the tunnel.

to solve the seepage problem, the following assumptions were made:

- the air pressure $u_a$ can be considered constant and equal to the atmospheric pressure;
- a linear relation (i.e. the Darcy's law) exists between the specific discharge $\mathbf{v}_w$ and the gradient of the hydraulic head $h$, being the hydraulic conductivity tensor $\mathbf{K}$ the proportionality coefficient;
- a relation exists between the degree of saturation $Sr$ and the soil suction $s$, the latter defined as the difference between pore air and pore water pressure $u_a - u_w$.

These assumptions were supposed to hold for the two porous media involved in the study, i.e. concrete and the surrounding soil, both assumed homogeneous and isotropic from the hydraulic point of view. In particular, a sandy soil was considered. The isotropic hydraulic conductivity was modelled as the product between the saturated conductivity $K_{sat}$ (constant for a given pore fluid and porosity) and the relative conductivity $K_{rel}$, which depends on the degree of saturation:

$$K = K_{sat} \cdot K_{rel}\ (Sr). \tag{2}$$

In particular, a widely accepted relationship for the relative permeability of sands was used (Ng and Menzies, 2007; Cosentini et al., 2012):

$$K_{rel} = Se^3, \tag{3}$$

being $Se$ the effective degree of saturation:

$$Se = \frac{Sr - Sr^{res}}{1 - Sr^{res}}. \tag{4}$$

$Sr^{res}$ is defined as the residual degree of saturation, i.e. the degree of saturation that remains in the soil after drying. The value of $Sr^{res}$ for the sandy soil analysed in this study was set equal to 0.045. As for the link between suction and degree of saturation, the classical van Genuchten water retention model was used (van Genuchten, 1980):

$$Se = \frac{1}{\left(1 + (\alpha s)^n\right)^m}, \tag{5}$$

being $\alpha$, $m$ and $n$ model parameters. In this study, typical parameters values for sandy soils were used: $\alpha$ = 0.36 kPa$^{-1}$, $n$ = 3.16, $m$ = 1–1/n (Zhu and Mohanty, 2002).

The hydraulic conductivity $K_{sat}$ for the saturated soil ($K_{sat,soil}$) was set equal to $10^{-4}$ m/s, based on the literature data (Leij et al., 1996).

As a first approximation the concrete was considered as a saturated porous medium, characterised from the hydraulic point of view just by a single parameter: the hydraulic conductivity ($K_{sat,concrete}$). In this paper, the hydraulic conductivity of the concrete, that is a priori unknown, was determined by means of inverse analysis by varying $K_{sat,concrete}$ in the range $10^{-9}$–$10^{-5}$ m/s,

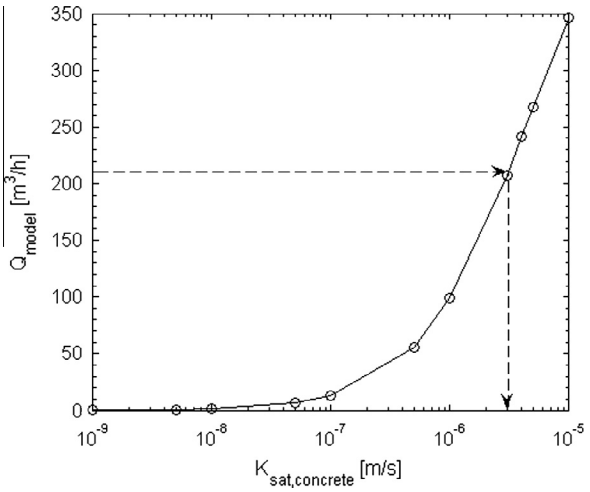


**Fig. 3.** Total water inflow into the tunnel estimated by the computational model as a function of the concrete hydraulic conductivity $K_{sat,concrete}$. The horizontal dashed arrow corresponds to the experimental water inflow ($Q_{exp}$ = 210 m$^3$/h) measured in the real tunnel.

being $10^{-14}$–$10^{-10}$ m/s the hydraulic conductivity range for the undamaged concrete (Luna et al., 2006; Oliver and Massat, 1992).

It is worth noting that the assumption of isotropic hydraulic response of concrete is a consequence of the isotropic nature of damage processes considered. Permeability anisotropy related to directional cracking is thus neglected. Moreover, this approach can be considered valid as long as the level of damage to which the tunnel lining is exposed is sufficiently far from the complete rupture conditions. In that case, one or several macrocracks are anticipated and they will govern fluid flow.

### 2.1.4. Initial and boundary conditions

Due to the time-dependence of the water mass balance equation for unsaturated porous media, initial distribution of pore water pressure at time $t = 0$ has to be set. In this case a hydrostatic distribution below and over the water table was chosen, being the water table located 13 m deep with respect to the ground surface.

As for the boundary conditions, a hydrostatic pressure distribution was maintained at the external vertical boundaries of the soil domain. For this purpose, the hydraulic head $h$ was set equal to the in situ value $h_{BC} = -13$ m, as measured by a piezometer placed at a known distance ($d$ = 50 m) from the tunnel. This corresponds to a phreatic surface located at a height $y_w$ = 3.3 m from the bottom of the tunnel, which is partially submerged. A datum placed at the ground surface has been chosen.

The bottom boundary of the soil was considered as impervious, whereas a constant suction condition was imposed on the upper boundary of the domain.

As for the internal perimeter of the tunnel below the phreatic surface, the water pressure $u_w$ was set equal to the atmospheric pressure. For the internal part of the tunnel above the phreatic surface, a no flux condition was applied on the tunnel internal perimeter. Since the position of the water table next to the tunnel is a priori unknown, it was determined by means of an iterative procedure.

### 2.1.5. Numerical discretisation

The equations discussed above were solved via the finite element method, by means of the commercial code Comsol Multiphysics 4.3b. (Comsol Inc, Burlington, MA, USA). The computational domain was discretized by the Comsol *Meshing tool* (Fig. 1b and c). Mesh sensitivity analysis led to the discretization of the domain with about 73,000 elements. Triangular elements were used in the tunnel area for a better discretization of the domain (Fig. 1c), whereas the remaining part of the soil domain was discretized by means of rectangular elements. Quadratic shape functions were used for the description of the nodal variable, i.e. the water pressure $u_w$.

## 2.2. Concrete hydraulic conductivity

As a result of the 2D finite element analysis, the amount of water inflow (per unit of length) per unit time q into the tunnel can be calculated as:

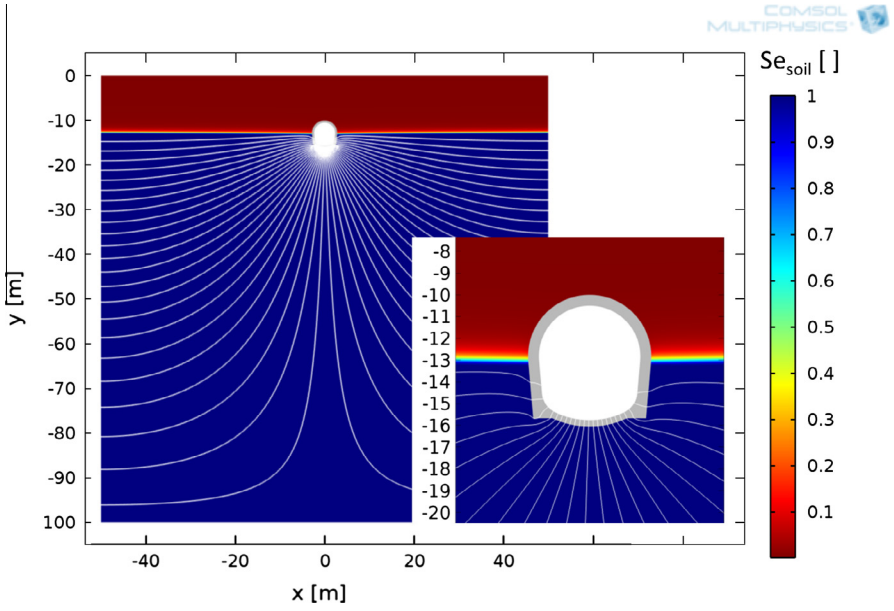


**Fig. 4.** Colour map of the soil effective degree of saturation (Se) and streamlines of the Darcy's velocity field. The water flow between each pair of adjacent streamlines is equal throughout the domain. A zoom detail of the computational domain nearby the tunnel cross-section is shown in the right box. Simulation parameters: $S_i$ = 0.3 m, $K_{sat,concrete} = 3.1 \cdot 10^{-6}$ m/s. (For interpretation of the references to color in this figure legend, the reader is referred to the web version of this article.)

$$q = -\int_{\partial A} \mathbf{v}_w \cdot \mathbf{n}\, ds, \tag{6}$$

where $\partial A$ denotes the tunnel internal boundary and $\mathbf{n}$ the unit normal vector in the outward direction. By the Darcy's law, $\mathbf{v}_w$ is calculated as $\mathbf{v}_w = -K_{\text{sat,concrete}} \nabla(y + u_w/\gamma_w)$, where $u_w$ is the water pressure, $\gamma_w$ the water specific gravity, $K_{\text{sat,concrete}}$ the hydraulic conductivity of the concrete, and $y$ the datum, expressed in accordance to the reference level. The value of $q$ is calculated for each concrete thickness class ($q_{\text{Si}}$). In order to obtain the overall water inflow for each class $S_i$, the flow contribution per unit of length ($q_{\text{Si}}$) was multiplied for the corresponding length $L_{\text{Si}}$. Finally, the total water inflow $Q_{\text{model}}$ of the segment is obtained by summing all the contributions of the different classes $S_i$:

$$Q_{\text{model}}\ (K_{\text{sat,concrete}}) = \sum_{S_i} q_{s_i}\ (K_{\text{sat,concrete}}) \cdot L_{S_i}. \tag{7}$$

The inverse analyses performed with different values of $K_{\text{sat,concrete}}$ allows the determination of a relation between the total water inflow and the concrete hydraulic conductivity. The value of hydraulic conductivity for which the total water inflow ($Q_{\text{model}}$) corresponds to the measured water inflow in the real tunnel ($Q_{\text{exp}}$ = 210 m$^3$/h, in the real case analysed) can thus be considered as the estimated value of $K_{\text{sat,concrete}}$.

## 3. Results

### 3.1. Concrete hydraulic conductivity

The evolution of $Q_{\text{model}}$ as a function of $K_{\text{sat,concrete}}$ is shown in Fig. 3. As expected, the lower the conductivity of concrete, the lower the water inflow per unit time in the tunnel. The comparison between $Q_{\text{model}}(K_{\text{sat,concrete}})$ and the experimental measurement of the water inflow $Q_{\text{exp}}$ allows determining the estimated value of the hydraulic conductivity of the concrete $K_{\text{sat,concrete}} = 3.1 \cdot 10^{-6}$ m/s.

The experimental measurement of water inflow $Q_{\text{exp}}$ has been obtained from the data collected in a draining well located at approximately halfway of the studied tunnel. The well was located at the point of minimum height of the track, and thus it seems reasonable to assume that it collects all the water seeping in through the concrete lining. It is worth noting that a careful visual inspection confirms that no water inflow is anticipated to occur in the tunnel segments adjacent to the studied one, so that they are not supposed to influence the measured value of $Q_{\text{exp}}$.

The colour map of the soil effective degree of saturation *Se* and the streamlines of the Darcy's velocity field obtained for a specific simulation setting (i.e. $S_i$ = 0.3 m, $K_{\text{sat,concrete}} = 3.1 \cdot 10^{-6}$ m/s) are shown in Fig. 4. The water table is located at an intermediate level of the tunnel cross-section, in accordance with the experimental evidence. The capillary fringe above the water table (i.e. the soil zone where the degree of saturation varies from about 90% to 100%) is less than 0.50 m, as expected for sandy soils. It is worth noting that the highest magnitude of the velocity field is located nearby the invert part of the tunnel cross-section, as shown by the highest density of the streamlines. This result is the direct con-sequence both of the highest hydraulic head gradient resulting in the soil region adjacent to the invert and of the lower thickness of the invert, with respect to the crown and sides of the tunnel.

### 3.2. Groundwater level variation

After the estimate of concrete hydraulic conductivity, the seepage model was used to assess the dependence of the total water inflow on the position of the phreatic surface. Different water table levels, expressed as the distance $y_w$ between the bottom of the tunnel and the water table, were simulated varying the hydraulic head $h_{\text{BC}}$ measured by the piezometer on the boundary. The relationship obtained between $Q_{\text{model}}$ and the water table level $y_w$ above the bottom of the tunnel is shown in Fig. 5. The model allows the prediction of the total water inflow when the water table level varies due to hydrogeological environmental conditions. In particular a quadratic relation between the water table level and the total water inflow was obtained.

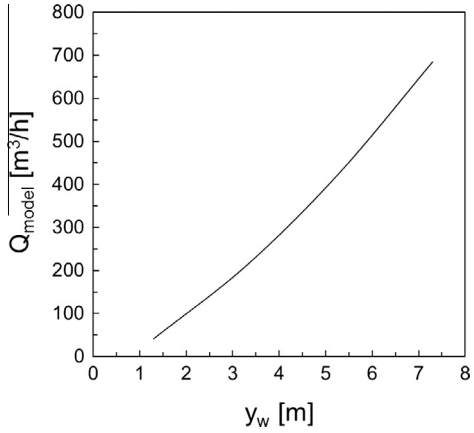


**Fig. 5.** Total water inflow estimated by the seepage model as a function of the water table height $y_w$ above the bottom of the tunnel. Simulation parameter: $K_{\text{sat,concrete}} = 3.1 \cdot 10^{-6}$ m/s.

## 4. Model reliability

In order to obtain some information about the reliability of the results of the method, an independent measure of concrete permeability, or other related properties, is needed. In this case, experimental data obtained by means of Mercury Intrusion Porosimetry (MIP) on five core samples retrieved from the invert of the studied tunnel was exploited. The location along tunnel length of the core-samples used for MIP is indicated in Fig. 2b). MIP is an experimental technique traditionally used to gather quantitative information on the microstructure of porous media with interconnected porosity. MIP is based on the application of an absolute pressure to a non-wetting liquid (mercury) in order to enter empty pores of a porous medium. Mercury intrusion is used to find the pore-size distribution of the investigated material, relating the volume of intruded pores to the pressure required for intrusion. A typical visualisation of MIP results includes the cumulative intruded vol-ume as a function of entrance or throat pore size. The intruded vol-ume normalised with respect to the total pore volume can be expressed through the cumulative function $F(R)$. The experimental results in terms of the evolution of the cumulative function $F$, as a function of pore radius $R$, are shown in Fig. 6a for one of the sam-ples analysed. The use of the logarithmic axis is due to the huge variation of pore radii in concrete.

Detailed information provided by MIP has been exploited by other authors (Romero and Simms, 2008; Romero et al., 2011; Della Vecchia et al., 2014) in order to estimate the water retention domain and the permeability of soils. $F(R)$ can be in fact identified with the current degree of saturation $Sr(R)$, which corresponds to a specific number of pores filled with water:

$$Sr(R) = F(R). \tag{8}$$

From the previous definition, it follows that, if all the pores are filled with water, the degree of saturation is equal to 1 and thus

$$Sr(R_{\max}) = F(R_{\max}) = 1. \tag{9}$$

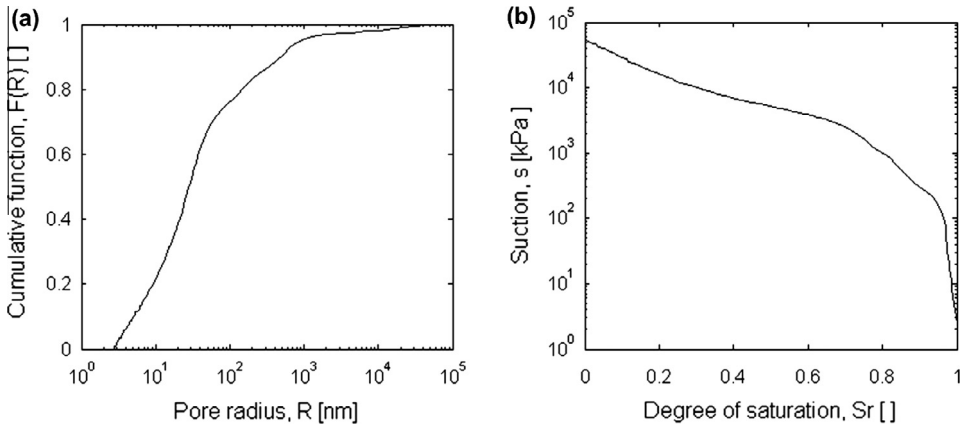


**Fig. 6.** Data obtained from Mercury Intrusion Porosimetry (MIP): (a) cumulative distribution of pore radius for a core sample of the concrete of the tunnel; (b) water retention curve for the concrete.

By means of the Laplace equation pore radius $R$ can be correlated to suction $s$:

$$s = \frac{2T\cos\theta}{r} = \frac{C}{r}, \tag{10}$$

where $T$ is the surface tension of water, and $\theta$ is the contact angle between water and soil particles.

The quantity $C = 2T\cos\theta$ is constant for a given mineralogy of the solid phase and chemical composition of the pore fluid. In this case, the values $T = 7.275 \cdot 10^{-2}$ N/m and $\theta = 0$ rad were chosen (Romero and Simms, 2008).

According to the previous equations, an estimate of the water retention curve can be obtained from MIP data. The water retention curve obtained for one of the concrete samples analysed in this study is shown in Fig. 6b. The concrete air-entry value (i.e. the suction value from which air starts to penetrate into the porous medium) estimated with the water retention curve is about 100 kPa (Fig. 6b), confirming the reasonability of the assumption of considering the concrete as saturated. In fact, the highest suction value on the tunnel lining obtained by the simulations was equal to 45 kPa (i.e. lower than the air-entry value of concrete).

According to the proposal of Brown et al. (1991), the hydraulic conductivity of a porous medium can be estimated by means of MIP through the equation

$$K_{\text{sat,concrete}} = \phi \frac{\rho_w g}{\mu} \frac{\langle r^2 \rangle}{8}, \tag{11}$$

where $\phi$ is the porosity of the concrete, $\rho_w$ and $\mu$ are the density and the dynamic viscosity of water, $g$ is the gravitational acceleration and $\langle r^2 \rangle$ is the second moment of the pore radius distribution. Concrete hydraulic conductivity estimated with this approach was compared with the $K_{\text{sat,concrete}}$ value back-estimated with the computational model. For the 5 concrete samples analysed in this study, $\phi$ and $\langle r^2 \rangle$ values calculated from the MIP data are equal to 14.3 ± 1.9% and 20.7 ± 8.3 μm$^2$, respectively. The concrete hydraulic conductivity obtained by using these values in Eq. (11) results $3.6 \cdot 10^{-6} \pm 1.4 \cdot 10^{-6}$ m/s, which is in accordance with the $K_{\text{sat,concrete}}$ value estimated with the computational model ($K_{\text{sat,concrete}} = 3.1 \cdot 10^{-6}$ m/s), thus proving the reliability of the proposed back-analysis.

## 5. Discussion and conclusions

The method proposed allows the study of water inflow in any underground tunnel to estimate concrete hydraulic conductivity, proposed as an index to evaluate the degradation of the tunnel lining. To implement the seepage model and perform the back-analysis to determine the permeability of the tunnel lining the following data are necessary: tunnel geometry and position with respect to the groundwater level; current thickness of the concrete; water inflow into the tunnel; hydraulic properties of the surrounding soil (i.e. hydraulic conductivity and retention curve).

All the needed properties can be quite easily collected for any tunnel considered. Data regarding the geometry of the tunnel and its position with respect to the ground surface are usually known from the plans supplied by the owner. The current lining thickness can be measured by means of non-destructive tech-niques: in this study GPR was used, which is a non-expensive experimental technique that permits a fast acquisition of thickness data with high accuracy. The velocity of data acquisition of GPR is particularly crucial during surveys of tunnel infrastructures, where the traffic cannot be interrupted for prolonged periods.

In case the GPR equipment was not available, the same method can be adopted by modelling tunnel sections with variable thickness in the range assumed as reasonable for the considered structure, with the limitation of obtaining as an outcome of the back analysis not a single value for the hydraulic conductivity but a range for $K_{\text{sat,concrete}}$.

In this study, the reduced thickness of the lining due to aging was considered only for the invert. However, if the survey of the infrastructure shows evident damage also of the crown or the sides of the tunnel, the parametric geometry proposed in this work can be easily modified allowing the simulation of different thickness values along the tunnel section.

As for the other information needed, the water table can be easily located by piezometers placed nearby the tunnel. The position of the piezometers is important as well, being necessary to the set in a consistent way the size of the computational domain. As for the total water inflow in the tunnel segment, it is usually recorded in the drainage wells in case of submerged underground tunnels.

Vice versa the choice of the hydraulic properties of the soil surrounding the tunnel can be a complicated task. Whilst the hydraulic conductivity of the soil can be easily obtained either by scientific literature, if the soil is known, or by in situ well pumping measurements, the water retention properties can create more difficulties. In this case dedicated water retention data were not available, thus literature data were exploited (Zhu and Mohanty, 2002). However, for the inverse method proposed to be robust and reliable, no dramatic changes of the estimated concrete permeability should be recovered as a consequence of the uncertainties related to the water retention properties of the surrounding soil.

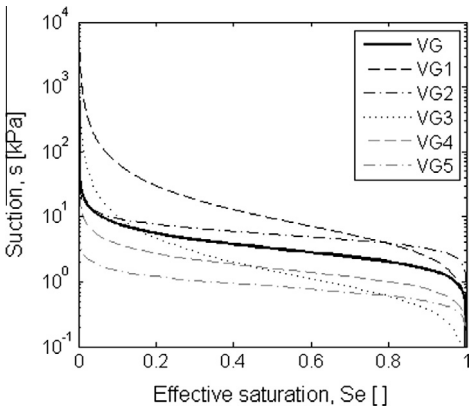


**Fig. 7.** Van Genuchten water retention curves for sandy soil. The solid line (VG) is the water retention curve used in the model for the back-analysis; the dashed lines represent the water retention curves used for the sensitivity analysis. VG: $\alpha = 0.36\ kPa^{-1}$, $n = 3.16$; VG1: $\alpha = 0.20\ kPa^{-1}$, $n = 1.89$; VG2: $\alpha = 0.20\ kPa^{-1}$, $n = 4.50$; VG3: $\alpha = 1.28\ kPa^{-1}$, $n = 1.89$; VG4: $\alpha = 0.74\ kPa^{-1}$, $n = 3.19$; VG5: $\alpha = 1.28\ kPa^{-1}$, $n = 4.50$.

**Table 2**
Results of the sensitivity analysis.

| Parameter Variation | $\Delta q\%$ |
|---|---|
| VG1 | 1.87 |
| VG2 | −0.39 |
| VG3 | −0.58 |
| VG4 | −0.74 |
| VG5 | −0.21 |

Output variations are expressed as percent change ($\Delta q\%$) with respect to the water filtration flow obtained in the reference case $q_{ref} = 13.53 \cdot 10^{-2}\ m^2/h$.
Parameters maintained constant: $K_{sat,soil} = 10^{-4}$ m/s, $S_i = 0.3$ m, $K_{sat,concrete} = 10^{-6}$ m/s, $h_{BC} = -13$ m, $W_d = 100$ m, $H_d = 100$ m.

To this aim, a sensitivity analysis of the model outcomes to input retention parameters was performed. A reference case was defined setting the geometrical and material properties as: $S_i = 0.3$ m, $K_{sat,concrete} = 10^{-6}$ m/s, $K_{sat,soil} = 10^{-4}$ m/s, $\alpha = 0.36\ kPa^{-1}$, $n = 3.16$. Soil retention curve parameters (i.e. $\alpha$, $n$) were then varied with respect to these reference values, in the range reported in the literature for sandy soils, as shown in Fig. 7. In particular, parameter $\alpha$ and n were set to range between 0.20 and 1.28 $kPa^{-1}$ and between 1.89 and 4.50, respectively (Ghanbarian-Alavijeh et al., 2010; Shaap and Leij, 1998). Five different sets of retention parameters (VG1, VG2, VG3, VG4 and VG5) were generated, whose effects in terms of water inflow q were compared to the value obtained in the reference case ($q_{ref}$), as shown in Table 2.

The effect of the variation of the van Genuchten curve parameters is almost negligible (lower than 1.9%): as expected, uncertainty in terms of retention properties is not critical for the implementation of the method, which proved to be sufficiently robust. The role of the unsaturated soil above the water table is in fact not crucial in terms of water inflow prediction for the materials considered, but it is crucial to allow a straightforward numerical solution of the unconfined seepage problem considered.

The sound agreement between concrete hydraulic conductivity obtained by the model and the experimental data obtained from MIP tests proves the reliability of the proposed approach. Core sampling to obtain MIP samples was performed in this study with the specific purpose of validating the computational model. The proposed method itself, in fact, can be applied to the study of any underground tunnel based on completely non-destructive procedures. Moreover, once determined the hydraulic conductivity of the damaged concrete, the model allows the prediction of the total water inflow as a consequence of water table level variations, allowing in time monitoring of the expected hydraulic state of the infrastructure.

The values ($K_{sat,concrete} = 3.1 \cdot 10^{-6}$ m/s) estimated for the concrete hydraulic conductivity by the model applied at the real tunnel examined in this study is remarkably higher than the values reported in the literature for the intact concrete (Luna et al., 2006). The obtained result is consistent with the data reported by Jeoung et al. (2008), who performed an experimental evaluation of the hydraulic conductivity of shotcrete lining core samples taken from a subsea tunnel. Based on the assumption that the permeabil-ity is a proxy for the level of damage of the concrete, our outcome denotes a severe damage of the analysed tunnel, as confirmed by the visual inspections performed in the tunnel and by the MIP analysis.

It is well known in fact that the hydraulic conductivity of a porous medium depends on several aspects related to the concrete state, like the size distribution and connectivity of the pores, as well as the presence of interconnected fissures and cracks. Despite in some cases concrete porosity has been considered as a significant index of damage (Kuhl et al., 2004a,b), the parameter $K_{sat,concrete}$ was here considered as a more significant property, depending not only on the quantity of voids itself, but also on several others connectivity and directional properties which can-not be linked to porosity (Oda, 1985; Shao et al., 2005; Maleki and Pouya, 2010). Even though hydraulic conductivity does not supply direct quantitative information about tunnel structural safety, the knowledge of this parameter can be important when monitoring the state of the underground structure. In this context, the method here proposed is a simple and effective tool to prioritize the maintenance works in underground tunnel lines.

## Acknowledgement

This study was funded by Politecnico di Milano, Young Research Grant 2012. Project Title: "Structural safety of underground infrastructures".

## References

Brown, P.W., Shi, S., Skalny, J.P., Grace, W.R., 1991. Porosity/permeability relationships. In: Skalny, J., Mindess, S. (Eds.), Materials Science of Concrete II. The American Ceramic Society Inc, Westerville, OH, pp. 83–109.

Choinska, M., Khelidj, A., Chatzigeorgiou, G., Pijaudier-Cabot, G., 2007. Effects and interactions of temperature and stress-level related damage on permeability of concrete. Cem. Concr. Res. 37 (1), 79–88.

Cosentini, R., Della Vecchia, G., Foti, S., Musso, G., 2012. Estimation of the hydraulic parameters of unsaturated samples by electrical resistivity tomography. Géotechnique 62 (7), 583–594.

Daniels, D.J., 2004. Ground Penetrating Radar, Second ed. Peter Peregrinus Ltd., London, U.K.

Della Vecchia, G., Dieudonne, A.C., Jommi, C., Charlier, R., 2014. Accounting for evolving pore size distribution in water retention models for compacted clays. Int. J. Numer. Anal. Meth. Geomech. http://dx.doi.org/10.1002/nag.2326. Ghanbarian-Alavijeh, B., Liaghat, A., Guan-Hua, Huang., Van Genuchten, M.Th., 2010. Estimation of the van Genuchten soil water retention properties from soil textural data. Pedosphere 20 (4), 456–465. http://dx.doi.org/10.1016/S1002-0160(10)60035-5.

Jeoung, J., Lee, S., Lee, G., 2008. Evaluation of hydraulic conductivity of shotcrete lining samples. World Tunnel Congress 2008. Underground Facilities for Better Environment and Safety – India, pp 1703–1710.

Kolymbas, D., Wagner, P., 2007. Groundwater ingress to tunnels – the exact analytical solution. Tunn. Undergr. Space Technol. 22, 23–27.

Kuhl, D., Bangert, F., Meschke, G., 2004a. Coupled chemo-mechanical deterioration of cementitious materials. Part I: Modeling. Int. J. Solids Struct. 41, 15–40.

Kuhl, D., Bangert, F., Meschke, G., 2004b. Coupled chemo-mechanical deterioration of cementitious materials. Part II: Numerical methods and simulations. Int. J. Solids Struct. 41, 41–67.

Lee, I., Nam, S., 2001. The study of seepage forces acting on the tunnel lining and tunnel face in shallow tunnels. Tunn. Undergr. Space Technol. 16, 31–40.

Lee, S., Jung, J., Nam, S., Lee, I., 2006. The influence of seepage forces on ground reaction curve of circular opening. Tunn. Undergr. Space Technol. 22, 28–38.

Leij, F.J., Alves, W.J., van Genuchten, M.Th., Williams, J.R., 1996. Unsaturated Soil Hydraulic Database, UNSODA 1.0 User's Manual. EPA Report 600/R96/095. USEPA, Ada, OK.

Lualdi, M., Lombardi, F., 2014a. Combining orthogonal polarization for elongated target detection with GPR. J. Geophys. Eng. 11 (5). http://dx.doi.org/10.1088/1742-2132/11/5/055006.

Lualdi, M., Lombardi, F., 2014b. Significance of GPR polarisation for improving target detection and characterization. Nondestr. Test. Eval. 29 (4), 345–356. http://dx.doi.org/10.1080/10589759.2014.949708.

Luna, M., Arcos, D., Duro, L., 2006. Effects of grouting, shotcreting and concrete leachates on backfill geochemistry. SKB Rapport R-06-107, Enviros, Spain (ISSN: 1402-3091).

Machacek, J., Bartak, J., 2003. Prague, old town square: sewerage coupling chamber. Applications of geophysical methods in building structure diagnostic. In: Mares and Pospisil (Ed.), Proceedings of the 9th European Meeting of Environmental and Engineering Geophysics, CAAG, P-016, pp. 1–5.

Maleki, K., Pouya, A., 2010. Numerical simulation of damage–permeability relationship in brittle geomaterials. Comput. Geotech. 37, 619–628.

Ng, C.W.W., Menzies, B., 2007. Unsaturated Soil Mechanics and Engineering. Taylor & Francis e-Library, New York, ISBN 0-203-93972-7.

Oda, M., 1985. Permeability tensor for discontinuous rock masses. Gèotechnique 35 (4), 483–495.

Oliver, J.P., Massat, M., 1992. Permeability and microstructure of concrete: a review of modelling. Cem. Concr. Res. 22, 503–514.

Pijaudier-Cabot, G., Dufour, F., Choinska, M., 2009. Permeability due to the increase of damage in concrete: from diffuse to localized damage distributions. J. Eng. Mech. 135 (9), 1022–1028.

Rethore, J., Borst, R.D., Abellan, M.A., 2007. A two-scale approach for fluid flow in fractured porous media. Int. J. Numer. Meth. Eng. 71 (7), 780–800.

Romero, E., Simms, P.H., 2008. Microstructure investigation in unsaturated soils: a review with special attention to contribution of mercury intrusion porosimetry and environmental scanning electron microscopy. Geotech. Geol. Eng. 26 (6), 705–727.

Romero, E., Della Vecchia, G., Jommi, C., 2011. An insight into the water retention properties of compacted clayey soils. Géotechnique 61 (4), 313–328. http://dx.doi.org/10.1680/geot.2011.61.4.313.

Schaap, M.G., Leij, F.J., 1998. Database-related accuracy and uncertainty of pedotransfer functions. Soil Sci. 163, 765–779.

Shao, J.F., Zhou, H., Chau, K.T., 2005. Coupling between anisotropic damage and permeability variation in brittle rocks. Int. J. Numer. Anal. Meth. Geomech. 29, 1231–1247.

Shin, Y., Kim, B., Shin, J., Lee, I., 2010. The ground reaction curve of underwater tunnels considering seepage forces. Tunn. Undergr. Space Technol. 25, 315–324. The British Tunnelling Society and the Institution of Civil Engineers, 2004. Tunnel Lining Design Guide. Thomas Telford Ltd., London, UK.

Usman, M., Galler, R., 2013. Long-term deterioration of lining in tunnels. Int. J. Rock Mech. Min. Sci. 64, 84–89.

van Genuchten, M.Th., 1980. A closed-form equation for predicting the hydraulic conductivity of unsaturated soils. Soil Sci. Soc. Am. J. 44, 892–898.

Vanicek, I., Vanicek, M., 2007. The degree of deterioration of the tunnels in the Prague metro based on a monitoring assessment. Acta Geotech. Slov. 2, 35–47.

Xiang, L., Zhou, H., Shu, Z., Tan, S., Liang, G., Zhu, J., 2013. GPR evaluation of the Damaoshan highway tunnel: a case study. NDT and E Int. 59, 68–76.

Zhiaqiang, Z., Mansoor, Y.A., 2013. Evaluating the strength of corroded tunnel lining under limiting corrosion conditions. Tunn. Undergr. Space Technol. 38, 464–475.

Zhu, Jianting, Mohanty, Binayak P., 2002. Spatial averaging of van Genuchten hydraulic parameters for steady-state flow in heterogeneous soils: a numerical study. Vadose Zone J. 1, 261–272.